**Title**
Bromine oxide—ozone interaction over the Dead Sea

**Journal**
Journal of Geophysical Research, 106(D10)

**ISSN**
0148-0227

**Authors**
Matveev, Valeri
Peleg, Mordechai
Rosen, David
et al.

**Publication Date**
2001-05-27

**DOI**
10.1029/2000jd900611

JOURNAL OF GEOPHYSICAL RESEARCH, VOL. 106, NO. D10, PAGES 10,375–10,387, MAY 27, 2001

# Bromine oxide – ozone interaction over the Dead Sea

Valeri Matveev,[1] Mordechai Peleg,[1] David Rosen,[1] Dafna Siman Tov-Alper,[1] Kai Hebestreit,[2] Jochen Stutz,[3] Ulrich Platt,[2] Donald Blake,[4] and Menachem Luria[1]

**Abstract.** Atmospheric measurements were performed during a 1 month period in early summer of 1997 at the Dead Sea in Israel in an attempt to identify bromine monoxide BrO, and evaluate its effect on ozone chemistry. The differential optical absorption spectroscopy (DOAS) technique was utilized to identify and measure BrO present in the air masses. Concurrent to the DOAS measurements, continuous monitoring of $SO_2$, $NO/NO_x$,$O_3$, and CO was performed. Filter samples for aerosol analysis and whole air canister samples for bromocarbon analysis were also collected. The present paper reports the complete comprehensive data set of the measurements at the Dead Sea site and is a continuation to our preliminary communication [Heberstreit et al., 1999]. The more complete data now available enable a more detailed examination of the sources and mechanisms of the reactive halogen species and the presentation of new conclusions. The results showed a diurnal repeating cycle of $O_3$ and BrO variations, correlated with solar radiation and wind direction. During the elevated BrO events, where bromine oxide rose to daily maximum values often exceeding 100 ppt, a clear negative correlation with $O_3$ was observed. During these episodes, the $O_3$ regularly decreased from noontime levels of 50-80 ppb or higher down to 10-30 ppb and occasionally to levels below the detection limit of 2 ppb. The enhanced BrO levels were associated with southerly winds that are typical for the location during midday hours. This suggests that a possible source for the reactive bromine species is the interaction of atmospheric oxidants with bromide at the surface of the large salt pans located at the southern end of the Dead Sea. Research flights flown over the area showed that ozone destruction to levels well below the background values were observed over large areas of the Dead Sea Valley.

## 1. Introduction

The tourist guide to the Dead Sea Valley, the deepest land area on the face of the earth, about 400 m below sea level, suggests that the medical curing power of the local air is associated with the high bromine compound content of the air. The basis of this statement is not referenced to in any atmospheric measurement but to the fact that the Dead Sea (DS) is one of the world's richest sources of bromine. Because the Dead Sea is a closed body of water with a low rate of freshwater inflow and a very high rate of evaporation (400 cm $y^{-1}$ [*Alpert et al.*, 1997]), the water salinity is 12 times higher than that of normal ocean water. Dead Sea water contains (on average) 5.6 g bromide $L^{-1}$ and 225 g chloride $L^{-1}$ (Br/Cl ratio ≈ 0.025) [*Niemi et al.*, 1997] as compared to normal ocean water which contains 0.065 g $Br^- L^{-1}$ and 19 g $Cl^- L^{-1}$ (Br/Cl- ratio of 0.0034) [*Sverdrup et al.*, 1942], resulting in a Br enrichment factor (ERBr = ([Br]/[Cl])DS/([Br]/[Cl])SMOW) of 7 as compared to standard mean ocean water (SMOW). The waters of the Dead Sea has been reported as having a pH of about 6.5 and a strong buffering capacity (Dead Sea Works, private communication, 1997).

During research flights over the Dead Sea region performed by the Air Quality Laboratory of the Hebrew University in the early 1990s, it was observed that ozone levels dropped frequently to almost zero, indicating that certain depletion mechanisms were taking place. It was postulated that this phenomenon was possibly similar to the boundary layer ozone depletion events previously noted in the polar region and attributed to reactive halogen species, such as BrO [e.g., *Tuckermann et al.*, 1997; *Barrie and Platt*, 1997]. This phenomenon of complete boundary layer ozone depletion was first discovered about a decade ago and observed at several Arctic sites such as Alert, Canada [*Bottenheim et al.*, 1990]; Barrow, Alaska [*Sturges et al.*,1993], Spitsbergen, Norway [*Solberg et al.*, 1996], and Thule and Sondre-Stromfjord in Greenland [*Rasmussen et al.*, 1996]. Similar phenomena were reported also for several Antarctic stations: Syowa, between August and early October of 1989 [*Murayama et al.*, 1992], Neumayer [*Wessel et al.*, 1998; *Lehrer*, 1999], and Arrival Heights [*Kreher et al.*, 1997]. These ozone depletion episodes occur after polar sunrise, with ozone levels dropping from their normal 30 - 40 ppb level to below instrument detection values (< 2 ppb). Observations showed a striking anticorrelation between ozone and filterable bromine levels (f-Br), that is bromine compounds that can be collected on cellulose aerosol filters [e.g., *Barrie et al.*, 1988; *Lehrer et al.*, 1997].

The key species in the chemical mechanisms responsible for the destruction of boundary layer (BL) ozone are the halogen atoms X,Y and their oxide radicals XO and YO (X,Y = Cl, Br,

---

[1] Environmental Sciences Division, School of Applied Sciences, The Hebrew University, Jerusalem, Israel.

[2] Institut für Umweltphysik, Ruprecht-Karls University, Heidelberg, Germany.

[3] Department of Atmospheric Sciences, University of California, Los Angeles, California.

[4] Department of Chemstry, University of California at Irvine, Irvine California.

Paper number 2000JD900611.
0148-0227/01/2000JD900611$09.00

**Table 1.** Halogen Oxide Self-Reactions and Cross Reactions and Their Potential for Tropospheric Ozone Destruction in General, Assuming Appreciable Amounts of Different Halogen Oxides Being Present in the Atmosphere[a]

| | XO + YO | $k_{xi}$ $10^{-14}$ cm$^3$ s$^{-1}$ | Relative $k_{xi}/k_{BrO+BrO}$ | General Ozone Destruction Potential |
|---|---|---|---|---|
| 1 | ClO + ClO | 1.6 | 0.005 | small |
| 2 | ClO + BrO | 1390 | 4.3 | high |
| 3 | ClO + IO | 1300 | 4 | unknown |
| 4 | BrO + BrO | 320 | 1 | high |
| 5 | BrO + IO | 6900 | 22 | potentially very important |

[a]From *DeMore et al.* [1997]

I) [*Wayne et al.*, 1995; *Le Bras and Platt*, 1995; *Platt and Lehrer*, 1997; *Barrie and Platt*, 1997]. The presence of BrO has been unequivocally verified in the Arctic BL [*Hausmann and Platt*, 1994; *Tuckermann et al.*, 1997]. The halogen oxides are formed in the ozone destruction process as seen in reactions (1) and (2) below.

There are two main ozone-destroying cycles in the troposphere:

(R1) $X + O_3 \rightarrow XO + O_2$

(R2) $Y + O_3 \rightarrow YO + O_2$

(R3) $XO + YO \rightarrow X + Y + O_2$

The net result is

(R4) $2\,O_3 \rightarrow 3\,O_2$.

The halogen oxide self-reactions (X = Y) are well known to destroy ozone, but the halogen cross reaction combinations (X = Br, Y = Cl or I) would be considerably more effective. Table 1 shows the rate constants of the different halogen self-reactions and cross reactions as compared to the BrO + BrO self-reaction (*DeMore et al.* [1994] for $T$ = 298° K). The last column of Table 1 gives the ozone destruction potential in general, for the various self-reactions and cross reactions. Table 1 gives an idea of the potential influence that small amounts of IO could have.

The second reaction cycle involves the reaction of $HO_2$ with halogen oxides:

(R5) $XO + HO_2 \rightarrow HOX + O_2$

where $k_5$ (in units of $10^{-11}$ cm$^3$ s$^{-1}$) is 0.7, 4.5, and 8.4 for X = Cl, Br, I, respectively, followed by

(R6) $HOX + h\nu \rightarrow X + OH$,

(R7) $OH + CO$ (or VOC) $+ O_2 \rightarrow HO_2 + CO_2$ (or other product),

where VOC is volatile organic carbon. Together with (R1)/(R2) the net effect of the cycle ((R5), (R6), and (R7)) also leads to ozone destruction where (R5) usually will be the rate-determining step.

It is interesting to note that the halogen oxide self- reaction and cross reaction mechanism (R3) as well as the $HO_2$ mechanism ((R5) to (R7)) are of zero order in $O_3$ as long as the ozone concentration does not become too low (for details, see *Tuckermann et al.* [1997]). This is due to the fact that the rates of (R3) and (R5) which are rate limiting (rather than (R1)) are independent of the ozone level.

The total ozone loss rate-limited by the self-reactions and cross reactions of halogen oxides (Table 1) is therefore given by

$$-\frac{d}{dt}[O_3] = 2\cdot\sum_i([XO]\cdot[YO])_i\cdot k_{xi} + \sum_j [HO_2]\cdot[X_jO]\cdot k_j \text{ ,}$$

where $i$ denotes the XO-YO pairs as given in Table 1 and $j$ refers to the different halogens. Thus an XO-XO catalytic mechanism with 30 parts per trillion BrO could reduce ozone to levels below the detection limit of commercial ozone monitors (≈ 2 ppb) within roughly 2 days.

The present paper reports the complete comprehensive data set of the measurements at the Dead Sea site for the entire campaign period and is a continuation to our preliminary communication [*Hebestreit et al.*, 1999]. Data are presented for the first time regarding volatile organic bromine, bromide, and chloride content of the air masses. Additionally, we have also examined the extent of the ozone depletion effect over the Dead Sea region by performing upper air flight measurements. The more complete data now available enable a more detailed examination of the sources and mechanisms of the reactive halogen species and the presentation of new conclusions.

## 2. Experiment

During the period from May 26 though June 21, 1997, a comprehensive set of atmospheric trace gas measurements and other relevant meteorological parameters were performed at a site in the Dead Sea Valley, Israel. The measurements were made from the Hebrew University mobile laboratory situated on a dam between the northern and southern part of the Dead Sea. Figure 1 indicates the location of the measurement site. This special position was chosen because of its proximity to the salt pans, which were assumed to act as major natural sources of halogen compounds. The main salt pans are located in the Dead Sea Valley some 23-25 km to the south-southwest of the measurement site. Consequently, detection of atmospheric halogen species was expected especially for southerly wind flows (see Figure 1). However, in principle, halogen compounds might also be released from the highly concentrated seawater under varying wind directions. The area of the measurement is quite remote from intensive human activities. A regional highway is located along the Dead Sea about 1 km from the site and a tourism center with several hotels is located 4-5 km to the south of the site. A possible interference may be due to industrial halogen

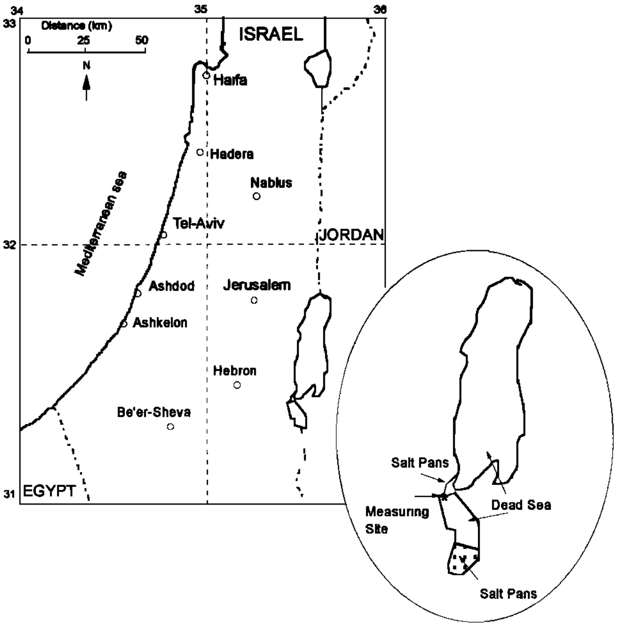

**Figure 1.** A map of central Israel and the location of the observation site at a dam on the Dead Sea.

sources which might arise from emissions of the Dead Sea Works factory, located about 22 km south of the measurement site.

The instrumental equipment included a differential optical absorption spectroscopy (DOAS), [see, e.g., *Platt et al.*, 1979; *Platt* 1994], high-sensitivity $SO_2$ and NO-$NO_x$ analyzers, $O_3$ and CO monitors, as well as continuous monitoring of the common meteorological parameters. During the measuring period, 94 canister samples were collected and then shipped to the University of California (Irvine) chemistry laboratory for the bromocarbon analyses using gas chromatography techniques with mass spectrometry and electron capture [*Blake et al.*,1999]. Samples for aerosol analysis were taken on a tandem Teflon/Nylon 47-mm filter pack. The sampled air passes first through the Nylon filter that retains gaseous nitrates and part of the sulfate, chlorides, and bromides. The second Teflon filter traps the remaining nitrate, sulfate, and halogen aerosols. The filter samples were collected on a 6-hour basis, for the time periods 0000-0600, 0600-1200, 1200-1800 and 1800-2400 local summer time (LST). The samples were later extracted in 10% metha-

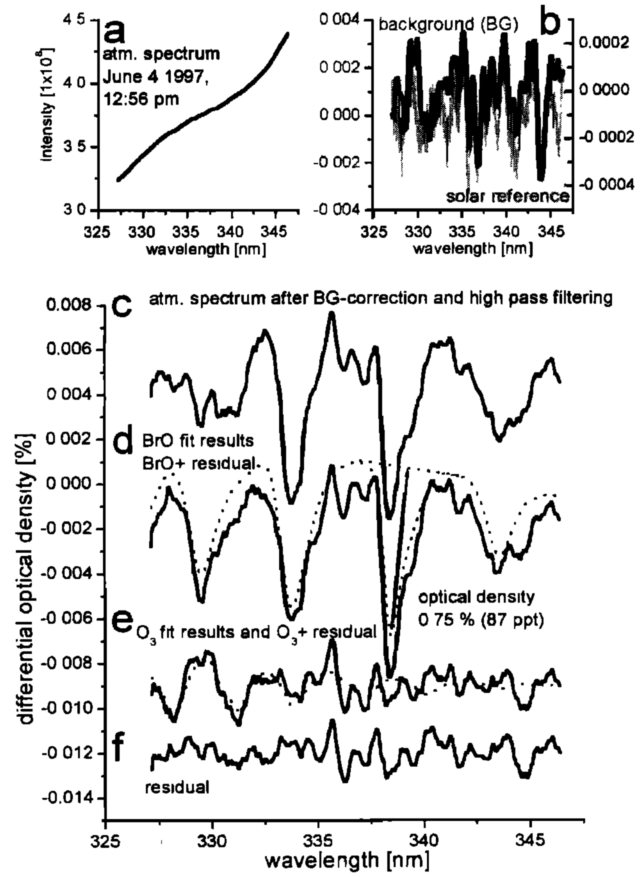

**Figure 2.** Analysis of a typical mid noon DOAS spectrum: A) atmospheric raw spectrum, B) background (BG) and solar reference (to underline the stray light compound of the BG), C) atmospheric spectrum after BG correction and band pass filtering D) BrO fit results and BrO + residual, arrow marks the differential optical density of the main absorption band E) $O_3$ fit results and $O_3$ + residual F) residual.

**Table 2.** List of Measurements at the Surface Site and on Board the Aircraft

| Parameter | Platform[a] | Operational Principal | Manufacturer | Detection Limit |
|---|---|---|---|---|
| BrO, $O_3$, $NO_2$ | G | DOAS | in house | 7 ppt, 20 ppb, 2 ppb |
| $SO_2$ | G | pulsed fluorescence | TEII 43S | 0.1 ppbv |
| NO | G, A | Chemiluminescence | TEII 42S | 0.1 ppbv |
| $NO_X$ | G, A | chemiluminescence + Mo converter | TEII 42S | 0.1 ppbv |
| $O_3$ | G, A | UV photometric | TEII 49 | 2 ppbv |
| CO | G | IR absorption | TEII 48 | 100 ppbv |
| Wind speed | G | 3-cup anemometer | Met-One 024A | 0.5 m $s^{-1}$ |
| Wind direction | G | Wind vane | Met-One 024A | 5° |
| Temperature | G, A | Thermistor | Met-One 060A | 0.4°K |
| Pressure | G, A | Transducer | MKS Baratron | 0.2 torr |
| Humidity | G, A | Capacitance | Met-One 083 | 3% |
| Halocarbons | G | gas-chromatograph, mass spectrometer, electron capture detectors | HP-6890 HP-5973 | 0.0001ppbV |
| $Br^-$, $Cl^-$, $NO_3^-$, and $SO_4^=$ | G, A | ion chromatograph | Dionex DX 500 | 0.1 μg $m^3$ |

[a] G = ground site, A = aircraft

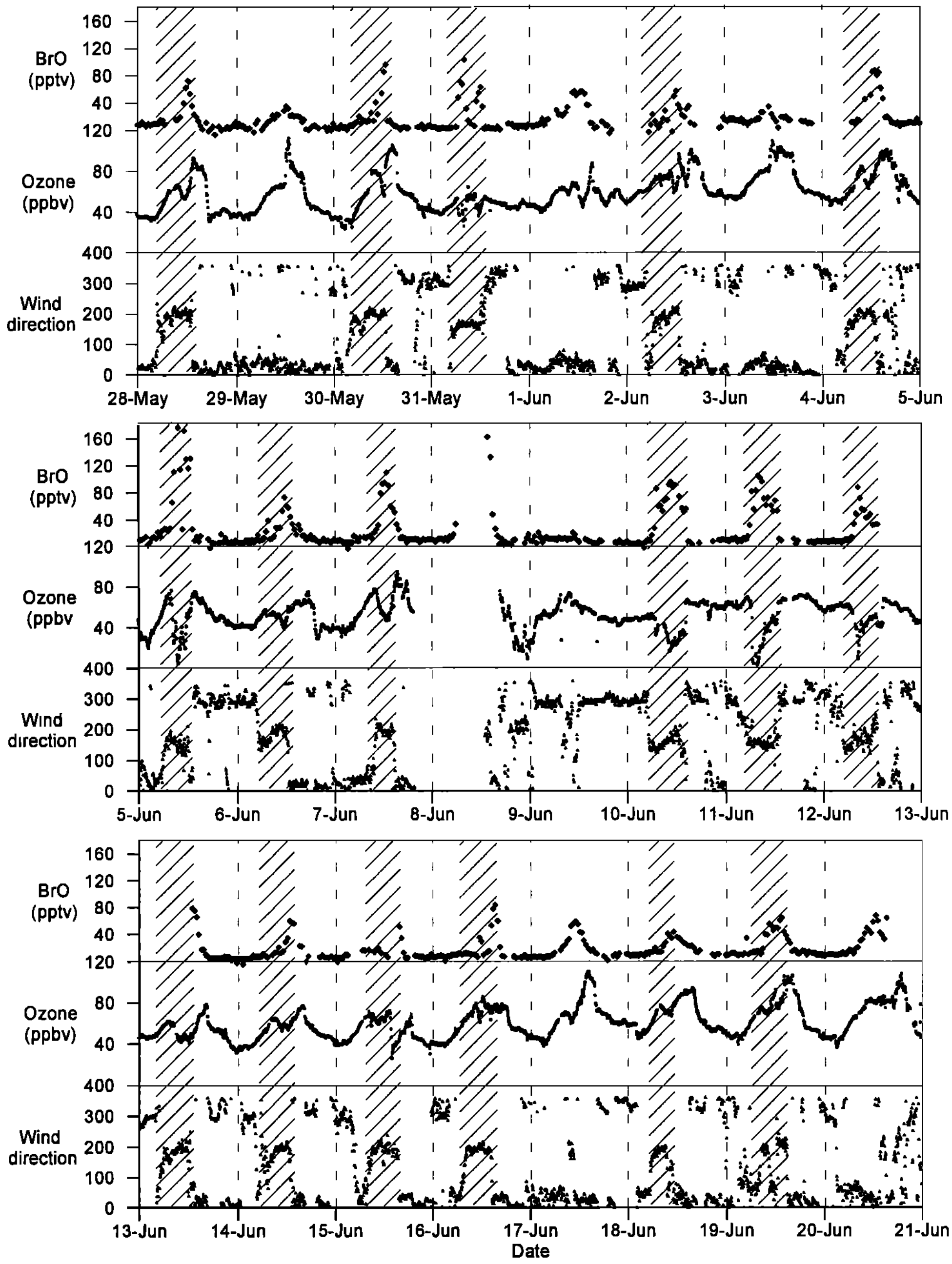

**Figure 3.** Time series of BrO (DOAS), $O_3$ and wind direction (in-situ) for the entire duration of the study (May 26 – June 21 1997). The shaded areas mark the periods of southerly wind flows (~135° to 225°). Major tick marks the given date.

**Table 3.** Summary of Aircraft Ozone Measurements Over the Dead Sea Basin[a]

| Minimum $O_3$ concentration Over the Dead Sea ,ppbv | Maximum Ozone Concentration, ppbv | Background Ozone Concentration, ppb | Takeoff Time, UT | Landing Time, UT | Date |
|---|---|---|---|---|---|
| < 2 | 156 | 45 | 1406 | 1638 | July 21,1997 |
| 60 | 161 | 60 | 1358 | 1603 | July 25. 1997 |
| (< 2) | (132) | (57) | (1441) | (1702) | (July 31, 1997) |
| < 2 | 107 | 50 | 1402 | 1603 | Aug. 1, 1997 |
| (< 2) | (130) | (54) | (1406) | (1606) | (Aug. 3, 1997) |
| < 2 | 161 | 68 | 1405 | 1626 | Aug. 7, 1997 |
| (< 2) | (135) | (61) | (1358) | (1620) | (Aug. 8, 1997) |
| < 2 | 150 | 63 | 1341 | 1553 | Aug. 10, 1997 |
| (75) | (237) | (65) | (1515) | (1743) | (Aug. 28, 1997) |
| 36 | 188 | 58 | 1341 | 1608 | Aug. 29, 1997 |

[a] Flights shown in Plate 1 are in parentheses.

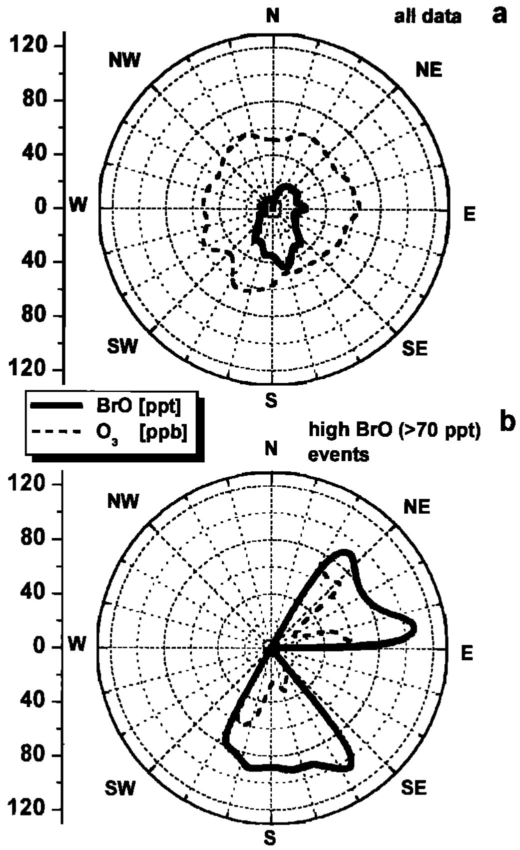

**Figure 4.** Distribution of BrO and $O_3$ concentrations as a function of wind direction. Shown are average values over 10 degree segments. The upper panel (A) shows all data, while the lower panel (B) shows only the periods of high BrO mixing ratios (BrO > 70 ppt). The scale on the left side indicates mixing ratios of BrO (ppt, thick line) and $O_3$ (ppb, dashed thin line), respectively.

nol-water mixture and analyzed for anions using ion chromatography [*Luria et al.*, 1996]. The filter data presented is the sum for both filters. Detailed descriptions of the instruments, and their minimum detection limits, are given in Table 2.

Ten research flights were performed during the afternoon hours between July 21 and August 29, 1997, over central Israel and the Dead Sea. The flights were performed at low altitudes of 300 m above surface level, well within the mixed layer. The instruments on board a Cessna 210 single engine aircraft included monitors for $O_3$ and $NO$-$NO_x$ as well as a global positioning system (GPS), temperature, humidity, and pressure sensors, and a filter package similar to the system used at the surface site. Aircraft instrumental details are also given in Table 2. Both the surface and aircraft measurements were recorded with a 10-s time resolution, and averaged over 1-m periods using a datalogger computer system.

DOAS measurements of BrO, $O_3$, and $NO_2$ were performed by analyzing the absorption structures of these species in the wavelength region of 337±10 nm, with a spectral resolution of 0.25 nm. The instrument consists of two Newtonian telescopes for emitting and receiving a light beam, a spectrograph, and a detector unit. The lamp (high-pressure Xe-arc lamp, Osram XBO 450W) with the transmitting telescope ($f$= 265 mm, diameter = 300 mm) was set up on a rooftop. The receiving telescope ($f$= 1800 mm, diameter = 300 mm), spectrograph, and detector unit was placed inside the mobile laboratory. The spectrograph was a 0.5-m Czerny-Turner instrument (Spex 1870C, 600 g $mm^{-1}$) with a slotted disk spectral scanning device as detector [*Platt and Perner*, 1984; *Platt*, 1994]. The optical path was oriented in a north-south direction with a length of 3.75 km.

The wavelength to channel relation (dispersion) varied over time due to the limited thermal stabilization of the spectrograph. However, it is possible to correct for these variations in the dispersion by comparing the spectral information of the absorbing species in the relevant spectral region of 327 - 347 nm (Figure 2a) to recorded mercury atomic emission lines, and the clearly visible (during daytime) Fraunhofer structures observed from scattered sunlight in our spectra (Figure 2b). The evaluation procedure included the following steps. The first step included subtraction of the background spectrum followed by band-pass filtration (high pass; division by a polynomial of the ninth order; low pass; 5 times adjacent smoothing) of the resulting spectra. After shifting the spectra to correlate wavelength and channel number (to avoid the thermal effects as described above), a logarithm was performed. Using the analyzing software MFC [*Gomer et al.*, 1993], a nonlinear least squares fit was performed [*Stutz and Platt*, 1996] for three reference spectra (BrO [*Hoenninger*, 1999], $NO_2$ (self recorded), and $O_3$ [*Bass and Paur*, 1985]), a solar spectrum [*Kurucz*, 1984] and a typical scattered light spectrum. Concurrently, a polynomial of the fourth order was applied to the fitted spectra. Finally, the concentrations were calculated from the fit results adjusted for pressure and temperature variations. Figure 2 shows the evaluation of a typical midday spectrum, recorded on the June 4, 1997, at 12.56. Depending on visibility variations caused by aerosols in the atmosphere, the typical time resolution of the instrument was 30 min. Previous results and a comparison with literature BrO reference spectrum [*Wahner et al.*, 1988] demonstrated the unambiguous identification of this compound as previously reported [*Hebestreit et al.*, 1999]. The average detection limit for BrO using the present setup was 7 ppt BrO (ppt is parts per trillion and refers to a mole ratio of $10^{-12}$, in the present case, pmole BrO/mole air) was attained using a light path of 3.75 km. The sensitivity for $NO_2$ and $O_3$ by the DOAS method was limited by the small absorption cross sections in the observed wavelength region (detection limit 2 ppb and 20 ppb, respectively). Because of the availability of independent in situ monitor data, none of these data are presented in this publication.

## 3. Results

The time series of BrO (DOAS), in situ $O_3$, and wind direction data for the entire research period, May 26 to June 21, 1997, are shown in Figure 3. BrO was observed for almost every day during the measuring period. In the present study, no attempt was made to identify the presence of ClO and IO due to present instrumental limitations. The BrO concentrations rose above background levels (around 10 ppt) during the late morning hours, peaking around noon before returning to background levels at around 1600 hours local summer time (LST = UT+3). The highest value recorded during the research campaign was 176 ppt. This value is the highest mixing ratio ever measured in the atmosphere, higher by a factor of 6 as compared to concentrations measured in polar regions and in the stratosphere. Ozone concentration varied from maximum values of above 120 ppb down to values below the detection limit of the instrument (2 ppb) during high BrO events at noontime.

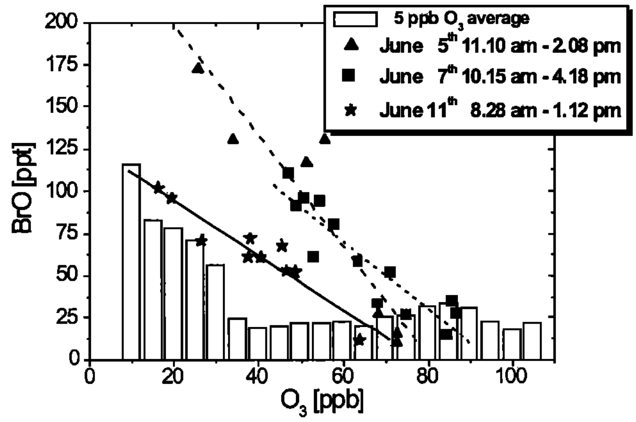

Figure 5. BrO – $O_3$ scatter plot. Only data above the detection limits of 7 ppt BrO and 2 ppb $O_3$ are considered. Three examples of elevated BrO events are shown and their corresponding linear fits. June 5th are shown as triangles and dash dot dash line, June 7th as squares and dashed line and June 11th as stars and a solid line. The entire data set is segmented into 5 ppb $O_3$ intervals represented by bars.

Elevated BrO levels were observed usually during southerly wind directions (135-225°, represented by shaded areas in Figure 3). Examination of the diurnal wind direction pattern in Figure 3 shows that during the nighttime and morning hours the wind flowed from the northerly direction. At around 1000 LST (0700 UT) the wind direction changed and started flowing from the south. This southerly wind direction continued until the late afternoon, around 1700 LST (1400 UT), when the wind flow was from the north once again. The above pattern was consistent for the entire study except for 4 days when the wind flowed from the north during the entire 24-hour period. The spatial variation and extensive BrO formation occurring during the southerly wind flows are shown in Figure 4. The overall spatial distribution of $O_3$ and BrO concentrations appear in Figure 4a and the distribution restricted to elevated BrO values (above 70 ppt) appear in Figure 4b. The $O_3$ depletion during the high BrO events in the southern sector is especially emphasized.

A BrO-$O_3$ scatterplot is shown in Figure 5. The plot shows all the data points for $O_3$ and BrO (above their respective detection limits of 2 ppb and 7 ppt), BrO averaged over increasing 5 ppb $O_3$ segments, represented as bars, in addition to regression lines for 3 different days. The strong negative correlation between BrO and ozone is quite distinct.

The results for the organic bromide compounds ($CH_3Br$, $CH_2Br_2$, and $CHBr_2Cl$) from the 94 canister samples taken, are shown in Figure 6 on a time series basis. The mixing ratio of $CH_3Br$ varied between 10 and 100 ppt, while the $CH_2Br_2$ and $CHBr_2Cl$ levels were below 10 ppt and 20 ppt, respectively. The daytime $CH_2Br_2$ values were higher, by about 50%, compared to the nighttime values, while the $CH_3Br$ and $CHBr_2Cl$ showed no diurnal variations.

The $O_3$ observations from the 10 flights taken during this study are given in Table 3. The ozone maximum values over the central parts of Israel during this period were always above 100 ppb and reached a maximum of more than 240 ppb in one case. These high values relate to photochemical smog typical for central Israel during the summer months. Background levels, outside the urban plume travel path, varied between 45 and 68 ppb. In contrast, over the Dead Sea on 7 of the 10 measuring days the $O_3$ levels were below the detection limit of the instrument (2 ppb).

## 4. Discussion

### 4.1. Ozone-BrO Interaction

During the measurement period BrO was observed on almost every day while mid-day $O_3$ decreases were observed during most of the sampling days (Figure 3). Ozone depletion was always accompanied with elevated BrO levels. No correlation was found between NO and $O_3$ levels, thus eliminating the possibility of ozone depletion by titration with fresh NO emissions. Furthermore, the $NO_x$ concentrations were quite low (generally below 10 ppb). Hence the $O_3$ depletion phenomenon can be assumed to be associated solely with Br catalyzed $O_3$ destruction ((R1) – (R3), X = Br).

As stated previously, during most of the measurement campaign the diurnal wind pattern was consistent, with northerly winds most of the time except during midday periods when southerly winds prevailed. Because the valley is relatively narrow (at most 30 km) and the terrain on its eastern and western boarders is quite elevated (more than 1 km above the sea surface on the east and almost 500 m at the west), the predominance of south and north wind directions are obvious. Due to the charac-

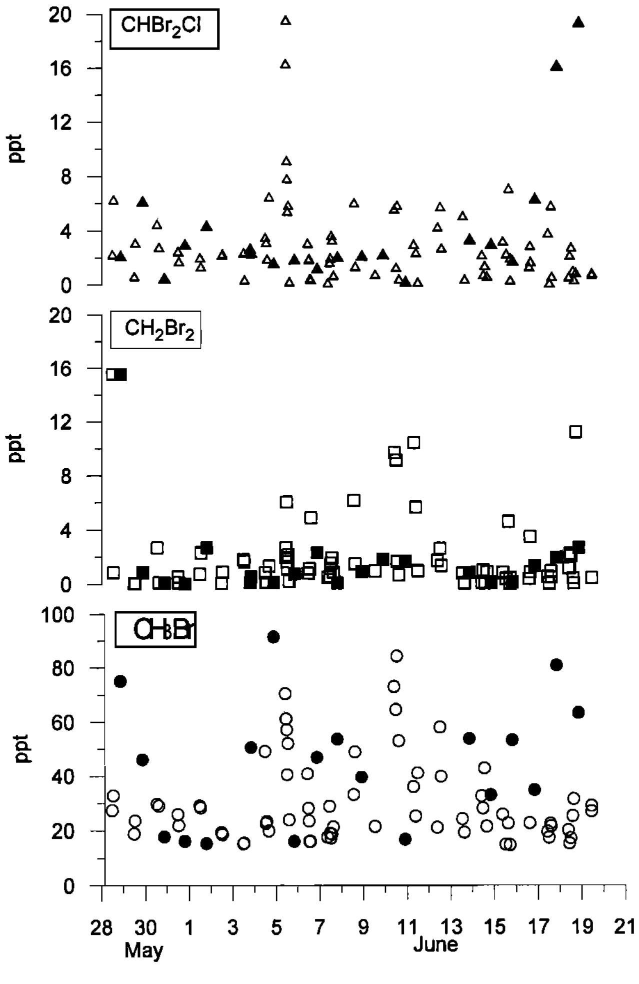

Figure 6. Mixing ratios of $CH_3Br$ (circles), $CH_2Br_2$ (squares), and $CHBr_2Cl$ (triangles) as determined from grab samples during the measuring period (May 26 to June 21). The open symbols represent daytime measurements (0800-2000 LST, 0500–1700 UT) and the solid symbols represent nighttime data.

teristics of the wind pattern during the measuring campaign, almost all the days with BrO peaks were associated with southerly winds.

Figure 7a, for June 5, 1997, illustrates a typical day when the wind flowed from the south during the midday hours (0900 – 1500 LST). The daily chemistry and meteorology cycle at the site are shown in the figure. On that day the highest BrO level was observed (176 ppt) with concurrent $O_3$ mixing ratios below detection limits. A brief pollution episode, with sharp increase of the $SO_2$ and $NO_2$ levels, was noted at around 1300 LST. This pollution peak is most probably related to emissions from the Dead Sea Works factory located south of the measuring site. It is evident from Figure 7a that the pollution episode lasted for no more than 30 min and was much shorter than the BrO-$O_3$ event that continued for about 5 hours.

Figure 7b (June 1, 1997) is an example of one of the few days when the wind direction remained from the north. Elevated BrO levels of up to 57 ppt were observed in the middle of a day even when the wind direction shift did not occur and the airflow remained northerly throughout the entire day. The midday BrO peak is evident, although significantly lower and a limited $O_3$ depletion event was observed. The pollution levels ($SO_2$, $NO_2$, NO) were moderate, again eliminating the possibility of association of the $O_3$ depletion with anthropogenic sources.

### 4.2. Sources of Reactive Halogen Species (RHS) at the Dead Sea

Since reactive halogen species (RHS) such as bromine appear to be responsible for the ozone depletion episodes, it is important to identify the sources of the RHS at the Dead Sea site. The environmental conditions at the Dead Sea are extremely different from those existing in the high Arctic during polar sunrise, where $O_3$-BrO reactions have previously been observed. The temperature is about 40°-50°C higher, ice surfaces do not exist, and high breaking waves are not present. Possible potential sources may include anthropogenic emissions such as bromine from the Dead Sea industries and bromine release from the Dead Sea itself and/or from sources within its vicinity.

**4.2.1. Anthropogenic emissions.** One potential source might be due to anthropogenic emissions from the bromine production plant at the Dead Sea Works. The plant produces $Br_2$ by the reaction of $Cl_2$ with Dead Sea solid extracts. The potential air pollution contribution of the Dead Sea Works on the measuring site can be calculated using basic dispersion equations. For the calculation of an upper limit impact value, the following assumptions were made: (1) emission rate of $Br_2$ to the air of 0.1 kg $h^{-1}$, (2) the highest possible atmospheric stability category during the midday hours (Pasquill-Gifford category D), (3) a wind speed of 2 m $s^{-1}$, and (4) wind flows directly from the plant to the site.

Based on these assumptions, the highest possible mixing ratio of total gaseous bromine compounds at the sampling site was calculated to be less than 1 ppt. Moreover, the Dead Sea Works also emits $SO_2$ and $NO_x$ showing a sharp peak (30 min duration, see Figures 7a and 7b) in contrast to the longer and broader peak of BrO. These two observations are consistent with anthropogenic pollutants emitted from a point source, while the BrO data suggest a release from a broad area source. Last, an anthropogenic source located 22 km south of the site cannot impact the site during days of continuous northerly winds.

**4.2.2. Liberation from sea salt by Br catalysis.** Several heterogeneous processes have been proposed to explain the release of RHS from a sea salt reservoir [*Fan and Jacob*, 1992; *Mozurkewich* 1995; *Sander and Crutzen* 1996; *Vogt et. al.,* 1996]. The most probable process of RHS liberation at the Dead Sea is the "bromine explosion" mechanism [*Lehrer et al.*, 1997; *Fan and Jacob*, 1992; *Tang and McConnell*, 1996] based on the uptake of HOBr on acidic salt surfaces:

(R8) $BrO + HO_2 \rightarrow HOBr + O_2$,

followed by

(R9) $HOBr + Br^-_{(aq)} + H^+_{(aq)} \rightarrow Br_2 + H_2O$.

The $Br_2$ molecule returns to the gas phase where it is quickly photolyzed to single halogen atoms,

(R10) $Br_2 + h\nu \rightarrow 2Br$.

The resulting halogen atoms are then immediately oxidized (R1). This ozone destroying sequence can be summarized as the bromine catalyzed net reaction:

(R11) $Br^-(aq) + H^+(aq) + HO_2 + 2O_3 \rightarrow BrO + H_2O + 3O_2$.

The above reaction sequence has been demonstrated in the laboratory [*Fickert et al.*, 1999; *Kirchner et al.*,1997]. One HOBr can release up to 2 Br atoms per cycle, where the second halogen atom is derived from the oxidation of the $Br^-$. As a consequence, the number of gas phase containing bromine molecules can increase exponentially (at the expense of $Br^-$ in the liquid layer on the salt surface), leading to an exponential growth of the BrO concentration. The above is true assuming that less than 50% of the bromine is lost from the reactive cycle by, for example, reaction of Br with $HO_2$ or $CH_2O$.

As can be seen from (R11), an acidic environment is required to promote the oxidation of $Br^-$ by HOBr. *Fickert et al.* [1999] have shown that this reaction proceeds only at $pH \leq 6.5$. As stated above, the pH of the Dead Sea water is at least 6.5 and is a strongly buffered solution.

The bromine explosion chemistry as described above requires initiation by a primary activation of reactive bromine compounds. Three different mechanisms are possible: bromine release via (1) $NO_x$ species or (2) ozone (see section 2.3) and do not require sunlight, or (3) the degradation of organohalogen compounds (see section 2.5) that proceeds only under daylight conditions. These potential start-up mechanisms are described below. On the other hand, the bromine explosion leads to an exponential growth of RHS species. Consequently, very low concentrations of bromine could trigger the reaction chain that is summarized as (R11).

**4.2.3. Liberation from sea salt by reaction of $NO_x$.** Two other heterogeneous halogen release mechanisms, the direct $NO_y$ (includes $NO + NO_2 + NO_3 + N_2O_5 + HNO_3$) or the $O_3$ release mechanisms, respectively, might cause the nighttime generation of RHS, reservoir species such as $XNO_2$. The above will be photolyzed after sunrise, forming RHS.

Under conditions of high $NO_x$ concentrations, the reaction of nitrogen oxides with NaCl, KBr, and other salt surfaces is known to release and $XNO_2$ [*Behnke et al.*, 1992, 1993; *Finlayson-Pitts and Johnson*, 1988; *Zetzsch and Behnke*, 1993], for example, via the following reaction:

(R12) $N_2O_5 + NaX \rightarrow NaNO_3 + XNO_2$.

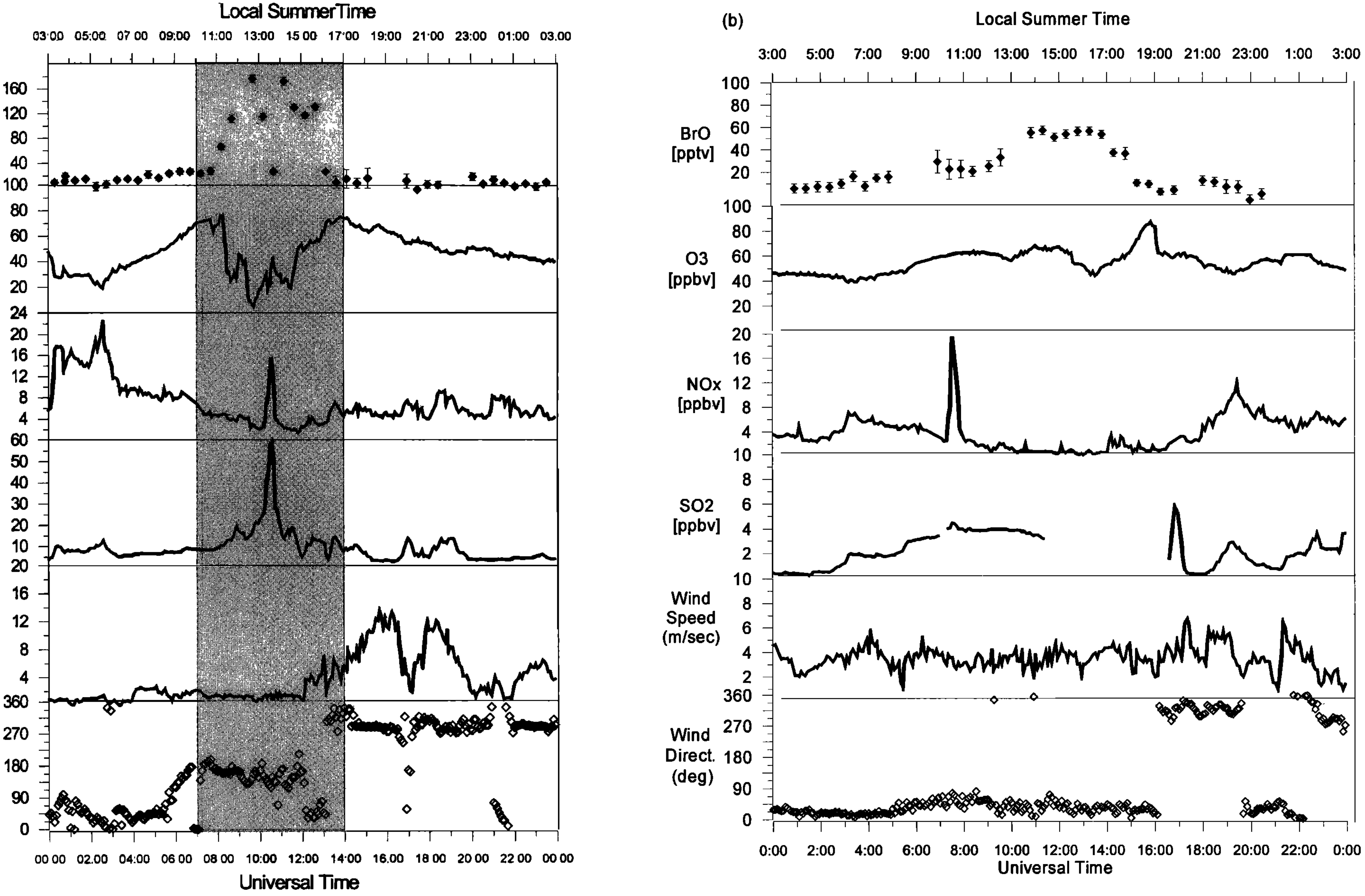

**Figure 7.** Mixing ratios of BrO, $O_3$, $SO_2$, $NO_2$ wind speed and wind direction as observed on (a) June 5 and (b) June 1, 1997. The error limits for BrO are also marked as vertical bars. Note the shift in wind direction from northerly to southerly and back during the middle of the day and the sharp industrial emission peak at 1000 UT, (LT = UT+3h) for June 5.

$XNO_2$ is rapidly photolzsed by sunlight [*Wayne et al.*, 1995] releasing halogen atoms. It also may react directly with the sea salt [*Schweitzer et al.*, 1999]:

(R13) $XNO_2(g) + NaX(s) \rightarrow NaNO_2(s) + X_2(g)$.

Up to the $XNO_2$ or $X_2$ formation stage, the mechanism proceeds without light and can lead to a "dark" source of reactive halogen molecules.

Another nighttime mechanism is the uptake of $NO_3$ by aqueous solutions of NaX:

(R14) $NO_3(g) + NaX(s) \rightarrow NaNO_3(s) + X(s)$.

The uptake coefficient of $NO_3$ by aqueous solutions of NaBr and NaCl was found by *Rudich et al.* [1996] to be near 0.01 for seawater. While *Gershenzon et al.* [1999] found an uptake coefficient up to 0.05 for dry NaCl. After sunrise, when the photolysis of $XNO_2$ and $X_2$ starts, a "burst" of XO should arise.

Another possible bromine activation mechanism has been suggested by *Oum et al.* [1998]. They suggested the reaction of ozone on the surface of seawater ice ($O_3 + Br^- \rightarrow BrO^- + O_2$) to produce the reactive species. The above reaction is, however, relatively slow. This reaction might also be operative at the surface of the salt pans and start the bromine release from the salt pans before sunrise. However, the $NO_x$ reactions mentioned previously ((R12), (R13), (R14)) are believed to be the dominant heterogeneous start-up mechanisms due to the relatively high $NO_x$ concentration present at the DS (see Figures 7).

**4.2.4. Influence of NO on RHS formation.** In parts of the troposphere affected by pollution, the reaction with NO is another source for bromine atoms shown in the following reaction:

(R15) $BrO + NO \rightarrow Br + NO_2$,

where $k_{15} = 1.7\times10^{-11}\ cm^3\ molec^{-1}\ s^{-1}$ (X = Cl) and $k_{15} = 2.1\times10^{-11}\ cm^3 molec.^{-1} s^{-1}$ (X = Br, I). Finally, the formation of bromine nitrate, $BrONO_2$:

(R16) $BrO + NO_2 \xleftrightarrow{surface} BrONO_2$

depends on the $NO_2$ concentration. Bromine nitrate is assumed to be quite stable against thermal decay but is readily photolyzed and may be converted to HOBr by heterogeneous hydrolysis:

(R17) $BrONO_2 + H_2O \xrightarrow{surface} HNO_3 + HOBr$

or to $Br_2$ or BrCl by heterogeneous reaction with HY (Y = Br, Cl):

(R18) $BrONO_2 + HY \xrightarrow{surface} HNO_3 + BrY$.

Overall, $BrONO_2$ is probably of minor importance at the low $NO_x$ levels typically found in the free troposphere but can play an important role in polluted air as occasionally found at the Dead Sea. A simple calculation suggests that, for typical conditions over the Dead Sea, most of the gas phase bromine should be in the form of $BrONO_2$. However, it is probable that in the present study the bromine nitrate was detected by the converter + chemiluminescence method and included in the general $NO_x$ term while not being detected by the other measurements techniques. From the present measuring campaign it is therefore not possible to identify the $BrONO_2$ contribution to BrO formation.

**4.2.5. Degradation of organohalogen compounds.** The last and probably least important source mechanism of halogen compounds at the Dead Sea is the degradation of organohalogens emitted by biological processes. These photolabile species are emitted by algae [e.g., *Carpenter et al.*, 1999; *Rasmussen et al.*, 1996; *Sturges et al.*, 1993; *Schall and Heumann*, 1993] and can act as precursors of halogen atoms in the troposphere. While many of these species are present in noticeable concentrations, that is $CH_3Br$ (Figure 6), the production rate of halogen atoms is small due to their slow reaction rate with hydroxyl (the photolytic lifetime of $CH_3Br$ is of the order of a year [*Yvon and Butler*, 1996]). This is the case for most compounds containing Cl and Br. In contrast, many of the organo-iodides have lifetimes of the order of hours or minutes and can contribute to iodine production even at low concentrations. Among the more photochemically active compounds are $CH_2I_2$ and $CH_2BrI$. Recent field measurements [*Carpenter et al.*, 1999] confirm the presence of these compounds in the boundary layer. Up to 1 ppt $CH_2I_2$ and $CH_2BrI$ have been measured at the Atlantic coast (Mace Head, Ireland). It is in principle possible that other, so far unidentified, short-lived organo-iodides contribute to iodine and bromine production. While *Tang and McConnell* [1996] suggested that only 3.5 ppt of bromoform could have been sufficient to initiate the autocatalytic bromine release, no distinct diurnal variation is evident for CH3Br and CH2Br2 (as seen in Figure 8). This would be necessary if organobromine compounds were to play the dominant role in RHS formation. Therefore, while the degradation of organobromides could be a start-up mechanism for the bromine explosion, it does not appear to be the main source of RHS.

### 4.3. Contribution of Different Sources of Atmospheric Bromine in the Dead Sea Valley

Figure 8 summarizes the diurnal variations of the various bromine and chlorine containing species: $CH_3Br$, $CH_2Br_2$, $CHBr_2Cl$ (canister grab samples), BrO (DOAS measurements), filterable bromine and chlorine (6-hour time segments filter samples) as measured at the Dead Sea site in 1997. All the data are presented as four distinct 6-hour averaged time periods, 0000-0600, 0600-1200, 1200-1800 and 1800-2400 (LST = UT+3). The filterable $Cl^-$ levels ranged from 100 to 1000 ppt as compared to 10 to 60 ppt for $Br^-$. The ratio between $Br^-$ and $Cl^-$ as obtained from the filter samples reflected the relative ratio between these ions in the Dead Sea water (molar ratio of 1:100 as compared with a molar ratio of approximately 1:90 observed for the Dead Sea waters [*Niemi et al.*, 1997]). As observed in Figure 8, the bromine content of the aerosol phase, bromocarbons, and BrO are all within the same order of magnitude, that is equivalent to 5 – 100 ppt of gas phase Br. However, only BrO shows a clear diurnal cycle, while the median levels of aerosol bromides and bromocarbons are essentially unchanged. The contribution to BrO from the photolysis of $CH_3Br$ and $CH_2Br_2$ cannot account for the observation because their photolysis lifetimes are of the order of months (Scientific Assessment of Ozone Depletion: 1998) [*World Meteorological Organization* 1998].

The concentration of bromine compounds in the aerosol phase was found to be too low to be considered as a significant source for the observed BrO. It is highly unlikely that the concentration of $Br^-$ in the potential source (the aerosol) will be equal to that of the observed BrO. This low and relatively constant aerosol content is not surprising since the Dead Sea near the sampling site is rather shallow (~10 m) and except for short periods (less

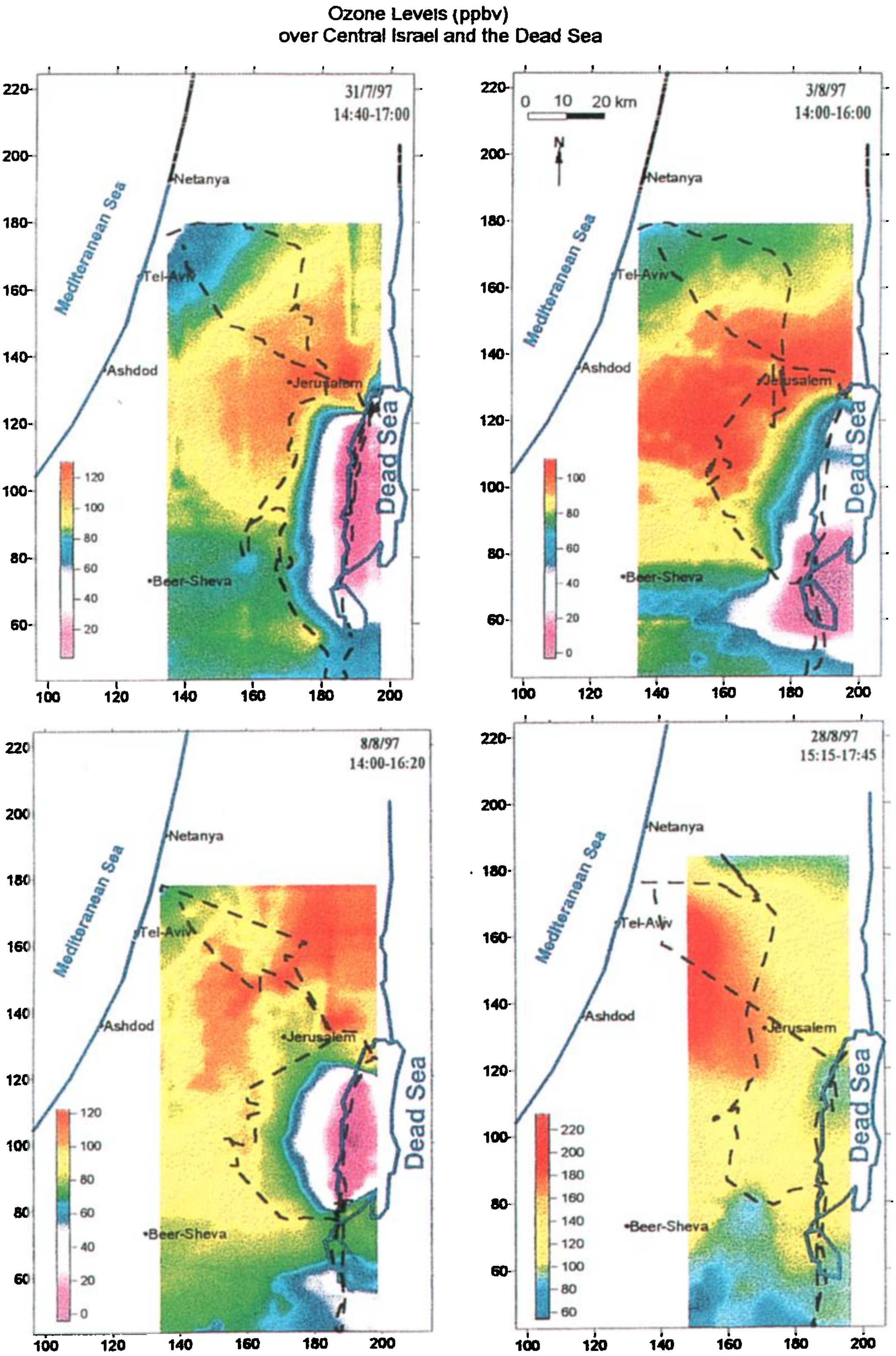
Ozone Levels (ppbv)
over Central Israel and the Dead Sea

**Plate 1.** Image plots of $O_3$ mixing ratios over Israel observed during four sampling flights. Note the $O_3$ depletion over the dead Sea Valley on three of the four sampling flights (the white and violet colors) on July 31, August 3, and 8, 1997. The dashed line represents the flight path.

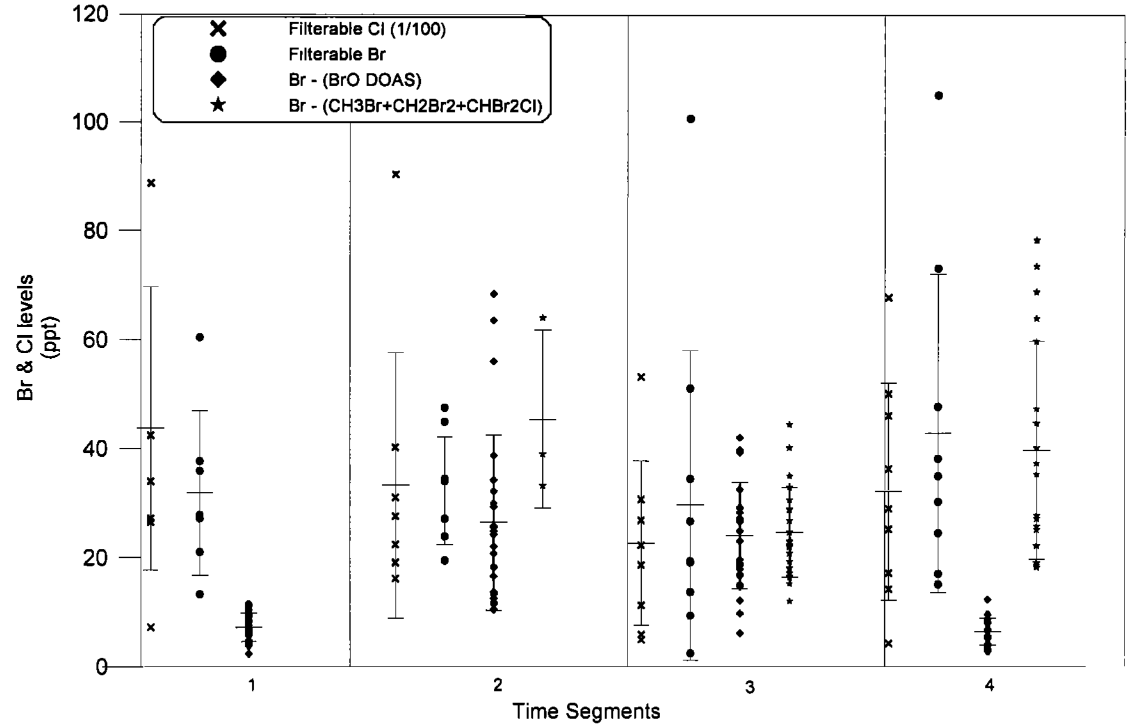

**Figure 8.** Comparison between the bromine species sampled: Average diurnal profiles of gas phase BrO, filterable bromine, $CH_3Br$, and $CH_2Br_2$. The data are averages over the four time segments, 0000-0600, 0600-1200,1200-1800 and 1800-2400 LST (UT+3). Also shown are the $Cl^-$ concentrations (divided by a factor of 100). The vertical bar indicates the range of the standard deviation, the horizontal line indicates the average value.

than 2-3 days per month) the winds are light (< 3 m $s^{-1}$). Consequently, significantly strong sea waves, that are expected to generate aerosols, will only be observed during infrequent and short storm periods. The present study was not performed during those periods.

The autocatalytic reactions involving HOBr as described above (section 2.2) appears to be the most likely source of BrO. Whatever is the correct mechanism for the bromine release, the reactions occur either on the surface of the Dead Sea and/or the bromine rich salt deposits (salt pans) The topsoil areas around the water contain high concentrations of bromine-rich sea salt due to the periodically covering of the soil by seawater and the high salinity of the water. This is especially so for the southern part of the sea where the waters are shallow and the sea has receded from large areas enabling the development of both natural and manmade salt pans. The highest BrO levels were observed with southerly winds as compared to lower BrO levels when northerly winds prevailed during midday. This might possibly support the hypothesis that the salt pans are the main source of RHS, since the southerly salt pans are much larger than those situated to the north of the measuring site.

Simple photochemical model calculations indicate that the observed BrO levels are insufficient to cause the ozone depletion as measured at the site [*Stutz et al.*, 1999]. The BrO concentrations at the salt pans are therefore expected to be much higher (of the order of 1-2 ppb) than those measured at the DOAS site some 25 km north of the salt pans.

### 4.4. The Geographical Extent of the Ozone Destruction Phenomenon

While the airborne sampling flights during July and August 1997 (see Table 3) were not performed simultaneously with the surface measurement, they provide information on the regional dimension to the phenomenon. Plate 1 shows the estimated distribution of $O_3$ over central Israel for 4 out of the 10 flights. The Kriging method with a linear variogram was employed to generate the two-dimensional plots. The first case (July 31, 1997) shows that very low $O_3$ levels prevail over most of the Dead Sea Valley. In the second case (August 3, 1997) the phenomenon is limited to the southern part, centered over the location of the sampling site. In the third example (August 8, 1997) the $O_3$ is depleted only over the northern part of the Dead Sea and there is no depletion over the sampling site. In the fourth case (August 28, 1997), no $O_3$ depletion over the Dead Sea was observed. On that day, one of the more severe smog episodes occurred over Israel. The urban plume from the densely populated Tel Aviv metropolitan area drifted toward Jerusalem and the Dead Sea. The peak $O_3$ mixing ratio measured in the plume was almost 240 ppb. It is likely that on this day the anthropogenic pollution "overwhelmed" the phenomenon of BrO-catalyzed $O_3$ destruction.

## 5. Conclusions

High levels of BrO (up to 176 ppt, the highest concentrations ever seen anywhere in the atmosphere) were observed over the Dead Sea in Israel. These high BrO levels observed during midday coincide with a parallel decrease (frequently to below detection limits,< 2 ppb) in the $O_3$ concentration. Although there are some recent reports of indirect evidence for halogen-catalyzed $O_3$ destruction at midlatitudes [*Nagao et al.*, 1999] the present study is the first direct observation of its kind at a location outside of the polar regions. Airborne measurements of $O_3$ levels have shown that the midday $O_3$ depletion covers large areas over the Dead Sea Valley. The possibility of anthropogenic release of bromine from the Dead Sea Works located at the southern shores of the Dead Sea was examined and ruled out. It is suggested that the processes responsible for the release of active bromine compounds is a reaction between atmospheric oxidants with salt reservoirs around the Dead Sea. The autocatalytic reaction involving HOBr (the bromine explosion mechanism [*Platt and Lehrer*, 1997]) is suggested to be the most likely mechanism responsible for the observed phenomenon. The Dead Sea region would appear to be an excellent natural laboratory for further investigations of the BrO-$O_3$ chemistry.

## References

Alpert, P., H. Shafir, and D.Issahary, Recent changes in the climate of the Dead Sea Valley, *Clim. Change, 7*, 513-537, 1997.

Barrie, L.A., and U.Platt, Arctic tropospheric chemistry: Overview, *Tellus, 49B*, 450-454, 1997.

Barrie, L.A., J.W.Bottenheim, R.C.Schnell, P.J.Crutzen, and R.A.Rasmussen, Ozone destruction and photochemical reactions at polar sunrise in the lower Arctic atmosphere, *Nature, 334*, 138-141, 1998.

Bass, A.M., and R.J. Paur, The ultraviolet cross-section of ozone,' I, The measurements / atmospheric ozone, in *Ozone in the Atmosphere, Proceedings of the Quadrennial Ozone Symposium 1984*, edited by C. Czerefos and A. Ghazi, pp. 606-616, D. Reidel, Norwell, Mass., 1985.

Behnke, W., H.-U. Kruger, V.Scheer, and C. Zetzsch, Formation of $ClNO_2$ and HONO in the presence of $NO_2$, $O_3$ and wet NaCl aerosol, *J. Aerosol Sci., 23*, 933-936, 1992.

Behnke, W., V. Scheer, and C. Zetzsch, Formation of $ClNO_2$ and $HNO_3$ in the presence of $N_2O_5$ and wet pure NaCl- and wet mixed NaCl/$Na_2SO_4$-aerosol, *J. Aerosol Sci., 24*, 115-116, 1993.

Blake, N.J., et al., Influence of southern hemispheric biomass burning on mid-tropospheric distributions of nonmethane hydrocarbons and selected halocarbons over the remote South Pacific, *J. Geophys. Res. 104*, 16,213-16,232, 1999.

Bottenheim, J.W., L. W.Barrie, E. Atlas, L. E Heidt, H.Niki, R. A. Rasmussen, and P.B. Shepson, Depletion of lower tropospheric ozone during Arctic spring: The Polar Sunrise Experiment 1988, *J. Geophys. Res. 95*, 18,555-18,568, 1990.

Carpenter, L.J., W.T.Sturges, S.A. Penkett, P.S.Liss, B. Alicke B, K. Hebestreit, and U. Platt, Short-lived alkyl iodides and bromides at Mace Head, Ireland: Links to biogenic sources and halogen oxide production, *J. Geophys. Res. 104*, 1679-1689, 1999.

DeMore, W.B., S.P. Sander, D.M.Golden, R.F. Hampson, M.J. Kurylo, C.J. Howard, A.R. Ravishankara, C.E. Kolb, and J. Molina , Chemical kinetics and photochemical data for use in stratospheric modeling, Jet Propu;sion Laboratory Pub., NASA, 92-96, 1997.

Fan, S.-M. and D. J. Jacob, Surface ozone depletion in the Arctic spring sustained by bromine reactions on aerosols, *Nature, 359*, 522 – 524, 1992.

Fickert, S., J.W. Adams, and J. N. Crowley, Activation of $Br_2$ and BrCl via uptake of HOBr onto aqueous salt solutions, *J. Geophys. Res., 104*, 23,719-23,727, 1999.

Finlayson-Pitts B. J., and S. N. Johnson, The reaction of $NO_2$ with NaBr: Possible source of BrNO in polluted marine atmospheres, *Atmos. Environ. 22*, 1107-1112, 1988.

Gershenzon, M.Y., S. Il'in, N.G. Fedetov, and Y.M. Gershenzon, The mechanism of reactive $NO_3$ uptake on dry NaX (X = Cl, Br), *J. Atmos. Chem., 34*, 119-135, 1999.

Gomer, T., T. Brauers, F. Heintz, J. Stutz, and U. Platt, MFC User Manual V 1.98, Inst.fur Umweltphysik der Univ. Heidelberg, Heidelberg, Germany, 1993.

Hausmann, M. and U. Platt, Spectroscopic measurement of bromine oxide and ozone in the high Arctic during Polar Sunrise Experiment 1992, *J. Geophys. Res. 99*, 25,399-25,414, 1994.

Hebestreit, K., J. Stutz, D. Rosen, V. Matveiv, M. Peleg, M. Luria, and U. Platt, DOAS measurements of tropospheric BrO in mid latitudes, *Science, 283*, 55-57, 1999.

Hoenninger, G., Referenzspektren reaktiver Halogenverbindungen fur DOAS Messungen, Diplomarbeit am Inst. fur Umweltphysik, Univ. Heidelberg, Heidelberg, Germany, 1999.

Jenkin M.E., The photochemistry of iodine-containing compounds in the marine boundary layer, Environmental and Energy Rep. AEA-EE- 0405 Harwell, U.K., 1992.

Kurucz, R.L., I. Furenlid, J.Brault, and L. Testerman, Solar flux atlas from 296 to 1300 nm, Atlas 1, Nat. Sol. Obs., Kitt Peak, Ariz.,1984

Kirchner, U., T. Benter, and R.N. Schindler, Experimental verification of gas phase bromine enrichment in reactions of HOBr with sea salt doped ice surfaces, *Ber. Bunsenges. Phys. Chem., 101*, 975-977, 1997.

Kreher, K., P.V. Johnston, S.W. Wood, and U. Platt, Gound-based measurements of tropospheric and stratospheric BrO at Arrival Heights, Antarctica, *Geophys. Res. Lett., 24*, 3021-3024, 1997.

Le Bras, G., and U. Platt, A possible mechanism for combined chlorine and bromine catalyzed destruction of tropospheric ozone in the Arctic, *Geophys. Res. Lett., 22*, 599-602, 1995.

Lehrer, E., Das polare troposphorische Ozonloch. Dissertation University of Heidelberg, Heidelberg, Germany, 1999.

Lehrer, E., D. Wagenbach, and U. Platt, Chemical aerosol composition during tropospheric ozone depletion at Ny-Alesund / Svalbard, *Tellus, 49B*, 486-495, 1997.

Luria, M., M. Peleg, G. Sharf, D. Siman Tov-Alper, N. Schpitz, Y. Ben Ami, Z. Gawi, B. Lifschitz, A. Yitzchaki, and I. Seter, Atmospheric sulfur over the east Mediterranean region, *J. Geophys. Res., 101*, 25,917-25,930, 1996

Mozurkewich, M., Mechanisms for the release of halogens from sea-salt particles by free radical reactions, *J. Geophys. Res., 100*, 14,199-14,207, 1995.

Murayama, S., T. Nakazawa, M. Tanaka, S. Aoki, and S. Kawaguchi, Variations of tropospheric ozone concentration over Syowa station, Antarctica, *Tellus 44B*, 262-272, 1992.

Nagao, I., K. Matsumoto, and H. Tanaka, Sunrise ozone destruction found in the sub-tropical marine boundary layer, *Geophys. Res. Lett., 26*, 3377-3380, 1999.

Niemi, T.M., Z. Ben-Avrahem, and J.R. Gat, (Eds.) *The Dead Sea: The Lake and Its Setting, Oxford Monogr. Geol. Geophys.*, vol. 36, Oxford Univ. Press, New York, 1997.

Oum, K.W., M.J. Lakin, and B.J. Finlayson-Pitts, Bromine activation in the troposphere by the dark reaction of $O_3$ with seawater ice, *Geophys. Res. Lett., 25*, 3923-3926, 1998.

Platt, U., Differential optical absorption spectroscopy (DOAS), in *Air Monitoring by Spectroscopic Techniques, Chem. Anal. Ser.*, vol. 127, edited by M.W. Sigrist, pp.27-84, John Wiley, New York, 1994

Platt, U., and E. Lehrer, Arctic Tropospheric Ozone Chemistry, ARCTOC, final report of the EU Proj. *EV5V-CT93-0318*, CEC, Heidelberg, Germany, 1997.

Platt, U. and D. Perner, *Measurements of Atmospheric Trace Gases by Long Path Differential UV/visible Absorption Spectroscopy, Optical and Laser Remote Sensing, Springer Ser. Opt. Sci.*, vol. 39, edited by D.K. Killinger and A. Mooradian, pp. 95-105, Springer-Verlag, New York, 1984

Platt, U., D. Perner, and H. Potz, Simultaneous measurement of atmospheric $CH_2O$ $O_3$ and $NO_2$ by differential optical absorption, *J. Geophys. Res. 84*, 6329-6335, 1979.

Rasmussen, A., J. Havskov Sorensen, S. Killsholm, and I.S. Mikkelsen, Analysis of tropospheric ozone measurements in Greenland, ARCTOC, final report of the EU Proj. *EV5V-CT93-0318*, CEC, Heidelberg, Germany, 1996.

Rudich, Y., R. Talukdar, and A.R. Ravishankara, Reactive uptake of $NO_3$ on pure water and ionic solutions, *J.Geophys. Res., 101*, 21,023 – 21,031, 1996.

Sander, R., and P.J. Crutzen, Model study indicating halogen activation and ozone destruction in polluted air masses transported to the sea, *J. Geophys. Res. 101*, 9121-9138, 1996.

Schall, C. and K.G. Heumann, GC determination of volatile organoiodine and organobromine compounds in seawater and air samples, *Fresenius J. Anal. Chem. 346*, 717-722, 1993.

Schweitzer, F., P. Mirabel, and c. George, Heterogeneous chemistry of nytryl halides in relation to tropospheric halogen activation, *J. Atmos. Chem. 34*, 101-117, 1999.

Solberg, S., N. Schmidtbauer, A. Semb, and F. Stordal, Boundary layer ozone depletion as seen in the Norwegian arctic in spring, *J. Atmos. Chem., 23*, 301-332, 1996.

Sturges, W. T., R.C. Schnell, G.S. Dutton, S.R. Garcia, and J.A. Lind, Spring measurements of tropospheric bromine at Barrow, Alaska, *Geophys. Res. Lett. 20*, 201-204, 1993,

Stutz, J., and U. Platt, Numerical analysis and estimation of the statistical error of differential optical absorption spectroscopy measurements with least squares methods, *J.Appl. Opt. 30*, 6041-6053, 1996.

Stutz, J., K. Hebestreit, B. Alicke, and U. Platt, Chemistry of halogen oxides in the troposphere: comparison of model calculations with recent field data, *J. Atmos. Chem., 34*, 65-85, 1999.

Sverdrup, H.U., M.W. Johnson, and R.H. Fleming, *The Oceans, Their Physics, Chemistry and General Biology*, Prentice-Hall, Englewood Cliffs, N.J., 1942.

Tang, T., and J.C. McConnell, Autocatalytic release of bromine from Artic snow pack during polar sunrise, *Geophys. Res. Lett., 23*, 2633-2636, 1996.

Tuckermann, M., R. Ackermann, C. Goelz, H. Lorenzen-Schmidt, T. Senne, J. Stutz , B. Trost, W.Unold, and U. Platt, DOAS-observations of halogen radical- catalysed arctic boundary layer ozone destruction during the ARCTOC campaigns 1995 and 1996 in Ny-Alesund, Spitsbergen, *Tellus, 49B*, 533-555, 1997.

Vogt, R., P.J.Crutzen, and R. Sander, A mechanism for halogen release from sea-salt aerosol in the remote marine boundary layer, *Nature, 383*, 327-330. 1996.

Wahner, A., A.R. Ravishankara, S.P. Sander, and R.R. Fiedl, Absorption cross section of Br between 312 and 385 nm at 298 and 223 K, *Chem. Phys. Lett. 152*, 507-512, 1988.

Wayne, R. P., et al., Halogen oxides: Radicals, sources and reservoirs in the laboratory and in the atmosphere, *Atmos. Environ. 29*, 2675-2884, 1995.

Wessel, S., S. Aoki, P. Winkler, R. Weller, A. Herber, and H. Gernandt, Tropospheric ozone depletion in polar regions: A comparison of observations in the Arctic and Antarctic, *Tellus, 50B*, 34-50, 1998

World Meteorological Organization, Scientific Assesement of Ozone Depletion: 1998, Global Ozone Research and Monitoring Project *Rep. 44*, WMO, Geneva, Switzerland, 1998.

Yvon, S.A. and J.H. Butler, An improved estimate of the oceanic lifetime of atmospheric $CH_3Br$, *Geophys. Res. Lett., 23*, 53-56, 1996.

Zetzsch, C. and W. Behnke, Heterogeneous reactions of chlorine compounds in Global Environmental Change NATO-ASI Ser. Ser I, 7, 291-306, 291-306, 1993.

---

D.R. Blake, Department of Chemistry, University of California, Irvine, CA 92697-2025. (e-mail: drblake@uci.edu)

K. Hebestreit and U. Platt, Institut fur Umweltphysik, Ruprecht-Karls-University, INF 229, D69120, Heidelberg, Germany. (Kai.Hebestreit@iup.uni-heidelberg.de;pl@uphys1.uphys.uni-heidelberg.de)

M. Luria (corresponding author), V. Matveev, M. Peleg, D. Rosen, and D.SimanTov-Alper, Environmental Sciences Division, School of Applied Sciences, The Hebrew University, Jerusalem, Israel, 91904. (luia@vms.huji.ac.il; msmtvv@pluto.mscc.huji.ac.il; pelegm@pob. huji. ac.il)

J. Stutz, Dept. Atmospheric Sciences, UCLA, 7127 Math Sciences, Los Angeles, CA 90095-1565. (jochen@atmos.ucla.edu)

(Received April 3, 2000; revised August 15, 2000;
accepted September 6, 2000.)